

Quantum Annealing via Environment-Mediated Quantum Diffusion

Vadim N. Smelyanskiy,^{1,*} Davide Venturelli,^{2,3} Alejandro Perdomo-Ortiz,^{2,3} Sergey Knys, ^{4,3} and Mark I. Dykman^{5,†}

¹Google, Venice, California 90291, USA

²USRA Research Institute for Advanced Computer Science (RIACS), Mountain View, California 94043, USA

³NASA Ames Research Center, Mail Stop 269-1, Moffett Field, California 94035-1000, USA

⁴Stinger Ghaffarian Technologies Inc., 7701 Greenbelt Road, Suite 400, Greenbelt, Maryland 20770, USA

⁵Department of Physics and Astronomy, Michigan State University, East Lansing, Michigan 48824-2320, USA

(Received 5 January 2016; revised manuscript received 18 December 2016; published 10 February 2017)

We show that quantum diffusion near a quantum critical point can provide an efficient mechanism of quantum annealing. It is based on the diffusion-mediated recombination of excitations in open systems far from thermal equilibrium. We find that, for an Ising spin chain coupled to a bosonic bath and driven by a monotonically decreasing transverse field, excitation diffusion sharply slows down below the quantum critical region. This leads to spatial correlations and effective freezing of the excitation density. Still, obtaining an approximate solution of an optimization problem via the diffusion-mediated quantum annealing can be faster than via closed-system quantum annealing or Glauber dynamics.

DOI: 10.1103/PhysRevLett.118.066802

Quantum annealing (QA) has been proposed as a candidate for a speed-up of solving hard optimization problems [1–3]. Optimization can be thought of as motion toward the potential minimum in the energy landscape associated with the computational problem. Conventionally, QA is related to quantum tunneling in the landscape that is slowly varied in time [4]. It provides an alternative to simulated annealing, which relies on classical diffusion via thermally activated interwell transitions. It was suggested that the coupling to the environment would not necessarily be detrimental to QA [5–7].

Recently, the role of quantum tunneling as a computational resource has become a matter of active debate [8–13], as it is not necessarily advantageous compared to classical computational techniques, e.g., the path integral Monte Carlo method [14–16]. In addition, dissipation and noise can make tunneling incoherent, significantly slowing down [17] the transition rates that underlie QA.

In this Letter we show that dissipation-mediated quantum diffusion can provide an efficient additional resource for QA. We model QA as the evolution of a far-from-thermal-equilibrium multispin system, which is coupled to a thermal reservoir and is driven by a time-dependent field. The diffusion involves environment-induced transitions between entangled states. These states are delocalized coherent superpositions of multispin configurations separated by a large number of spin flips (a large Hamming distance). At a late stage of QA the diffusion coefficient decreases. Ultimately diffusion becomes hopping between localized states and QA is dramatically slowed down. An important question is whether the solution obtained by then is closer to the optimum than the solution obtained over the same time classically.

Diffusion plays a special role when the system is driven through the quantum critical region, as often considered in QA [2,4,8]. A well-known result of going through such a

region is the generation of excitations via the Kibble-Zurek mechanism [18,19]. This leads to an error, in terms of QA, as the system is ultimately frozen in the excited state. The generation rate can be even higher in the presence of coupling to the environment [20,21].

It is diffusion that makes it possible for the excitations to “meet” each other and to recombine, thus reducing their number. Near the critical region, diffusion is enhanced because of the large correlation length. It has universal features related to the simple form of the excitation energy spectrum.

The effect of quantum-diffusion-induced acceleration of QA is of the utmost importance for systems with delocalized multispin excitations, in particular, above or close to the threshold of many-body localization transition. To reveal and characterize this new effect, we study it here for a model with no disorder. This model is of interest on its own as an example of a far-from-equilibrium system coupled to the environment. The specific model is a one-dimensional Ising spin chain driven through the quantum phase transition by varying a transverse magnetic field at a constant speed. Among recent applications of this classic model, we could mention cold-atom systems [22–24] and the circuit QED [25].

We assume that each spin is weakly coupled to its own bosonic bath. The QA Hamiltonian is

$$H_{\text{QA}} = -J \sum_{n=1}^{N-1} (\sigma_n^z \sigma_{n+1}^z + g \sigma_n^x) - \sum_{n=1}^N \sigma_n^x X_n + H_B, \quad (1)$$

where N is the number of spins, $Jg(t)$ is the transverse field, σ_n^x , σ_n^z are Pauli matrices, $H_B = \sum_{n,\gamma} \hbar \omega_{\gamma n} b_{\gamma n}^\dagger b_{\gamma n}$ is the baths' Hamiltonian, $X_n = \sum_{\gamma} \lambda_{\gamma n} (b_{\gamma n}^\dagger + b_{\gamma n})$, and $b_{\gamma n}^\dagger$, $b_{\gamma n}$ are boson creation and annihilation operators in the n th bath. We assume Ohmic dissipation, $2 \sum_{\gamma} (\lambda_{\gamma n} / \hbar)^2 \delta(\omega - \omega_{\gamma n}) = \alpha \omega$, $\alpha \ll 1$, and a linear-in-time schedule for reducing the

transverse field, $\dot{g}(t) = -v < 0$, starting from the initial value $g_i \gg 1$. We further assume translational symmetry, so that $\lambda_{\gamma n}$ and $\omega_{\gamma n}$ are independent of n . The spin-boson coupling (1) provides a microscopic model for the classical spin-flip process in the Glauber dynamics [26].

In the absence of coupling to the environment, model (1) describes a quantum phase transition between a paramagnetic phase ($g > 1$) and a ferromagnetic phase ($g < 1$) [27]. The spin part of the Hamiltonian (1) can be mapped onto fermions [28] using the Jordan-Wigner transformation, $\sigma_n^x = 1 - 2a_n^\dagger a_n$, $\sigma_n^z = -K(n)(a_n^\dagger + a_n)$, where $K(j) = \prod_{i < j} \sigma_i^x$ and a_n^\dagger and a_n are fermion creation and annihilation operators. Changing in the standard way to new creation and annihilation operators η_k^\dagger , η_k , with $\eta_k = (1/\sqrt{N}) \times \sum_{n=1}^N [a_n \cos(\theta_k/2) - ia_n^\dagger \sin(\theta_k/2)] e^{-ikn}$, we obtain the Hamiltonian of the isolated spin chain as $H_0 = 2J \sum_k \epsilon_k \eta_k^\dagger \eta_k$, where ϵ_k is the dimensionless fermion energy,

$$\epsilon_k = \sqrt{(g - \cos k)^2 + \sin^2 k}, \quad \tan \theta_k = \frac{\sin k}{g - \cos k}. \quad (2)$$

The dependence of the minimal energy $\Delta = 2J\epsilon_0$ on g and the form of ϵ_k are illustrated in Fig. 1.

In the course of QA, pairs of fermions with opposite momenta are born from vacuum due to the Landau-Zener transitions as the system passes through the critical point $g = 1$ [18,19]. The resulting density of excitations n_{KZ} for large N is simply related to the QA speed [29],

$$n_{\text{KZ}} = |\hbar \dot{g} / 8\pi J|^{1/2}. \quad (3)$$

In terms of the fermion operators, the Hamiltonian of the coupling to bosons, Eq. (1), reads

$$H_i = \sum_{kk'} h_{kk'} X_{k-k'}, \quad (4)$$

$$h_{kk'} = c_{kk'} \eta_k^\dagger \eta_{k'} + s_{kk'} \eta_k^\dagger \eta_{-k'}^{\dagger} + s_{k'k}^* \eta_{-k} \eta_{k'},$$

where $X_q = \sum_\gamma \lambda_\gamma (b_{\gamma q} + b_{\gamma -q}^\dagger)$ are boson field operators, $b_{\gamma q} = N^{-1/2} \sum_n b_{\gamma n} \exp(-iqn)$, and the coefficients $c_{kk'}$ and $s_{kk'}$ are expressed in terms of the rotation angles θ_k , $\theta_{q'}$, see Eq. (24) of the Supplemental Material (SM) [30].

From Eq. (4) one can identify three types of relaxation processes, see Figs. 1(b)–1(c). The first is scattering by a boson in which a fermion changes its momentum k and energy ϵ_k . The rate of a single-fermion transition $k \rightarrow k'$ is $W_{kk'}^{+-} \propto |c_{kk'}|^2$. The other processes are generation and recombination of pairs of fermions due to boson scattering. The parity of the total number of fermions is not changed. The generation and recombination rates $W_{kk'}^{++}$ and $W_{kk'}^{--}$ are $\propto |s_{kk'}|^2$,

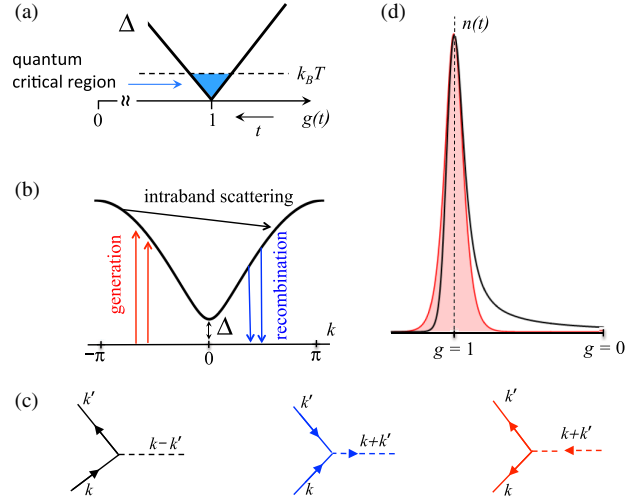


FIG. 1. (a) The dependence of the gap Δ in the energy spectrum of the Ising chain (2) on the scaled transverse field g , which linearly decreases in time. (b) The fermion dispersion law and the processes of fermion scattering induced by the coupling to the bosonic field. Both the generation and the recombination are two-fermion processes. (c) The diagrams that show single-fermion intraband scattering, recombination, and generation of fermions; the change of the fermion energy and momentum comes from the bosons. (d) The dependence of the density of quasiparticles on time ($g = 1 - \dot{g}t$). The boundary of the filled region shows the thermal equilibrium density, whereas the solid line shows the nonequilibrium density calculated using the Boltzmann equation (6) and disregarding spatial correlations.

$$W_{kk'}^{\mu\nu} = \frac{2\pi\alpha}{N} \Omega_{kk'}^{\mu\nu} [1 - \mu\nu \cos(\mu\theta_k - \nu\theta_{k'})] [\bar{n}(\Omega_{kk'}^{\mu\nu}) + 1],$$

$$\Omega_{kk'}^{\mu\nu} = 2J(\mu\epsilon_k + \nu\epsilon_{k'})/\hbar, \quad (5)$$

where $\mu, \nu = \pm$ and $\bar{n}(\omega) = [\exp(\hbar\omega/k_B T) - 1]^{-1}$.

The single-particle quantum kinetic equation that incorporated these processes was considered in Refs. [20,21]. It was written for the coupled fermion populations $\langle \eta_k^\dagger \eta_{k'} \rangle$ and coherences $\langle \eta_k \eta_{-k} \rangle$. The approach [20,21] involved two major approximations, the spatial uniformity of the fermion distribution and the absence of fermion correlations. These approximations hold in the critical region, where the gap in the energy spectrum $\Delta(g) = 2J|1 - g| \lesssim k_B T$. For a sufficiently low QA rate, the density of excitations is dominated by thermal processes rather than the Landau-Zener tunneling [20,21]. The fermion population in this region is $[\exp(2J\epsilon_k/k_B T) + 1]^{-1}$, see Fig. 1(d).

QA aims at minimizing the number of excitations over a given time. As we show, for the considered open system there exists an optimal QA speed that allows one to achieve the excitation density far below the Landau-Zener-limited density (3) in a closed system. This density corresponds to the bottleneck of QA imposed by the sharp slowing-down of excitation decay due to many-fermion effects and spatial correlations. The approximation [20,21] does not capture this effect. The full analysis requires solving the full Bogolyubov

chain of equations for the coupled many-particle Green's functions [38]. However, the density where the slowing-down occurs and the scaling relations between the speed \dot{g} and the final density of excitations, which are our primary interest, can be found in a simpler way, as discussed below.

As we show, the range of interest is g behind the critical region, yet close to it, where $1 - g \ll 1$. In this range, as g decreases, spatial correlations in the fermion system change from weak to strong. We start with the region of comparatively high densities, where spatial correlations can be disregarded and the fermion dynamics is described [39] by the Boltzmann equation for the single-fermion Wigner probability density $\rho_W(x, k) = (2\pi)^{-1} \int dp \langle \eta_{k+p/2}^\dagger \eta_{k-p/2} \rangle e^{-ipx}$,

$$\partial_t \rho_W + \frac{2J}{\hbar} (\partial_k \epsilon_k) \partial_x \rho_W = \hat{\mathcal{L}}^{(0)}[\rho_W] + \hat{\mathcal{L}}^{(1)}[\rho_W]. \quad (6)$$

Here, operator $\hat{\mathcal{L}}^{(0)}$ describes single-fermion scattering by bosons [39], see Fig. 1, with the transition rates $W_{kk'}^+$ given by Eq. (5); cf. Eqs. (6) and (9) in the Supplemental Material [30]. The characteristic reciprocal relaxation time of fermion momentum due to single-fermion scattering τ_r^{-1} is determined by the transition rate $W_{kk'}^+$ for fermions with energies $2J\epsilon_k, 2J\epsilon_{k'} \sim k_B T$,

$$\tau_r^{-1}(g) = 2\alpha k_B T [(1-g)/\beta g \hbar^2]^{1/2}, \quad \beta = 2J/k_B T. \quad (7)$$

This expression refers to the semiclassical range behind the critical point where the excitation gap Δ has become large compared to $k_B T$,

$$e^{-\Delta(g)/k_B T} \ll 1, \quad \Delta(g) = 2J(1-g). \quad (8)$$

The rate $\tau_r^{-1}(g)$ increases with the distance $1-g \propto \Delta$ from the critical point. Extrapolating it back to the critical region $\Delta \approx k_B T$, we recover the scaling of the critical relaxation rate $(\tau_r^{-1})_c$ found in [20,21]. For the slow quantum annealing rate that we consider,

$$J|\dot{g}| \ll \hbar(\tau_r^{-1})_c, \quad (\tau_r^{-1})_c \approx 4J\alpha/\hbar\beta^2, \quad (9)$$

the fermion distribution in the critical region remains of the Boltzmann form.

Operator $\hat{\mathcal{L}}^{(1)}[\rho_W]$ in Eq. (6) describes two-fermion generation and recombination accompanied, respectively, by absorption and emission of a boson, see Fig. 1. Recombination requires a collision of two fermions with a boson, see Fig. 1. Respectively, the recombination term is quadratic in ρ_W ,

$$\hat{\mathcal{L}}_{\text{rec}}^{(1)}[\rho_W(x, k)] = -N \sum_q W_{kq}^{++} \rho_W(x, k) \rho_W(x, q). \quad (10)$$

It becomes small for small fermion densities. In contrast, the generation term $\hat{\mathcal{L}}_{\text{gen}}^{(1)}[\rho_W(x, k)]$ is density-independent for small densities and is proportional to $W_{kq}^- \propto \exp[-\Delta(g)/k_B T]$. It rapidly falls off as the control parameter g moves away from the critical point.

Overall, in the range (8) the generation and recombination rates described by $\hat{\mathcal{L}}^{(1)}$ are small compared to the momentum relaxation rate τ_r^{-1} , and the distribution over the fermion momentum approaches thermal equilibrium with the bosonic bath temperature. Function $\rho_W(x, k)$ in (6) factors into a product of the Boltzmann distribution over fermion energy ϵ_k and a coordinate-dependent fermion density $n(x, t)$, $\rho_W = n(x, t) \exp(-\beta\epsilon_k) / \sum_k \exp(-\beta\epsilon_k)$.

A new time scale is associated with the decay of density fluctuations. In the considered approximation this decay is described by the diffusion equation

$$\dot{n}(x, t) = D \partial_x^2 n(x, t), \quad D = c_D \frac{J\beta^{1/2}}{\alpha\hbar} \frac{g^{3/2}}{(1-g)^{3/2}}. \quad (11)$$

The diffusion coefficient (11) has a standard form $D \sim \langle v_k^2 \rangle \tau_r$ with $v_k = (2J/\hbar) \partial_k \epsilon_k$ being the fermion velocity; D sharply increases with decreasing $1-g$. In Eq. (11) $c_D \approx 0.17$ [30].

On the time long compared to the decay time of density fluctuations, the distribution $n(x, t)$ becomes uniform and its evolution is determined by generation and recombination processes. The spatially averaged density $\langle n \rangle$ is described by a rate equation,

$$\langle \dot{n} \rangle = -w(\langle n \rangle^2 - n_{\text{th}}^2). \quad (12)$$

Here, $n_{\text{th}} \equiv n_{\text{th}}(g) = N^{-1} \sum_k \exp(-\beta\epsilon_k)$ is the thermal equilibrium density, whereas $w(g) = \sum_{k,q} W_{kq}^{++} \exp[-\beta(\epsilon_k + \epsilon_q)] / N n_{\text{th}}^2$ is the recombination rate. From Eq. (5), for $\beta \gg 1-g, 1/g$

$$w(g) \approx \frac{8\pi\alpha J}{\hbar\beta g}, \quad n_{\text{th}}(g) \approx \left(\frac{1-g}{2\pi\beta g} \right)^{1/2} e^{-\beta(1-g)}. \quad (13)$$

As $g \equiv g(t)$ decreases, the thermal density n_{th} exponentially sharply falls down. The mean density $\langle n \rangle$ cannot follow this decrease, so that the density of fermions becomes higher than the thermal density. This happens for the value $g(t) = g_{\text{th}}$ where the correction $\delta\langle n \rangle = \langle n(t) \rangle - n_{\text{th}}(g(t))$ becomes $\sim n_{\text{th}}(g(t))$, see Figs. 1 and 2. The quasistationary solution of the linearized Eq. (12) reads $\delta\langle n \rangle \approx -\dot{n}_{\text{th}}/2wn_{\text{th}}$. This gives an equation for g_{th}

$$\beta^{-1} w(g) n_{\text{th}}(g) = |\dot{g}| \quad \text{for } g = g_{\text{th}}. \quad (14)$$

As g is decreased below g_{th} and reaches the region $\exp\{\beta[g_{\text{th}} - g(t)]\} \gg 1$, we can disregard n_{th} in Eq. (12). Then using the explicit form of the rate $w(g)$, we obtain

$$\langle n(t) \rangle \approx \beta^{-1} n_{\text{th}}(g_{\text{th}}) (\log [g_{\text{th}}/g(t)])^{-1}. \quad (15)$$

This expression describes quantum annealing of fermion density in a strongly nonequilibrium regime. We observe that $\langle n(t) \rangle$ varies with time only logarithmically here.

For still smaller g , not only does the system move further away from thermal equilibrium in terms of $\langle n \rangle$, but it also

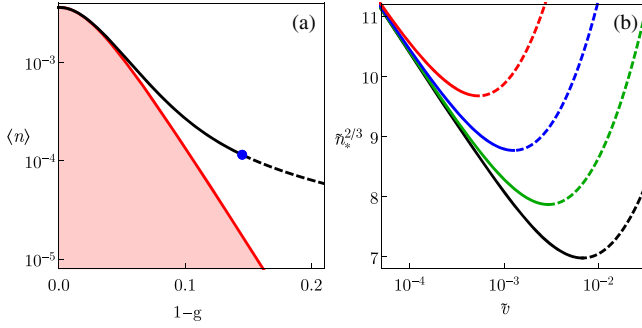


FIG. 2. Fermion density (a) vs the distance to the critical point and (b) vs the annealing rate. In (a), the filled region is bound by the thermal distribution $n_{\text{th}}(g)$. The black line shows the non-equilibrium density $\langle n \rangle$ for $\alpha = 0.06$, $\beta = 25$, and $|\dot{g}| = |\dot{g}|_{\text{opt}} = 2.85 \times 10^{-7}$, see Eq. (12). The blue point marks the crossover value g_* . For $g < g_*$ spatial correlations become strong and the theory is inapplicable. In (b), the red, blue, green, and black lines show the scaled density $\tilde{n}_* = c_d \beta^3 n_* / 8k\pi\alpha^2$ vs the scaled QA rate $v = \hbar\beta^3 |\dot{g}| / 4\sqrt{2\pi}J\alpha$ for $\log \mu = 8, 9, 10, 11$, respectively [parameter $\mu \propto (\beta/\alpha)^2$ is defined in (17)]. The minimal density $n_{\text{opt}} = \min n_*$. The dashed sections of the lines refer to the regions where the asymptotic theory does not apply.

develops strong spatial fluctuations. This is due to the sharp decrease of the diffusion coefficient $D = D(g)$, see Eq. (11). Spatial fluctuations of the density $n(x, t)$ impose a bottleneck on the recombination in one-dimensional systems [36], because for fermions to recombine they first have to come close to each other. In contrast to the usually studied reaction-diffusion systems, in the present case the bottleneck arises not because of the decrease of the density, but, in the first place, because of the falloff of the diffusion coefficient. Once the recombination becomes limited by diffusion, the change of the fermion density becomes slower than in Eq. (15).

To estimate the density $n_* = \langle n(t_*) \rangle$ where the crossover to diffusion-limited recombination occurs, we set the rates \dot{n} of the recombination and diffusion processes equal to each other. For the recombination, one can use Eq. (12), $\dot{n} = -wn^2$. For the diffusion, one can use Eq. (11) where the mean interparticle distance $1/\langle n \rangle$ is chosen as a spatial scale on which the density fluctuates. This gives

$$n_* = \langle n(t_*) \rangle = kw(g_*)/D(g_*), \quad g_* = g(t_*), \quad (16)$$

where $k \sim 1$. An alternative way of estimating n_* is described in Sec. IV of the SM [30].

Equations (14)–(16) relate the crossover value of $g = g_*$ to the value g_{th} where thermal equilibrium is broken. Since g_* , g_{th} are close to the critical point $g = 1$, it is convenient to switch to variable $z = \beta(1 - g)$, with $z_* = \beta(1 - g_*)$ expressed in terms of $z_{\text{th}} = \beta(1 - g_{\text{th}})$ as follows:

$$\mu(\beta/\alpha)^2 z_{\text{th}}^{1/2} \exp(-z_{\text{th}}) = z_*^{3/2} (z_* - z_{\text{th}}), \quad (17)$$

where $\mu = c_D/8k\sqrt{2\pi^3}$; note that $\beta/\alpha \gg 1$. Equations (14)–(17) express the crossover density n_* in terms of the speed $|\dot{g}|$.

Beyond the crossover point, $g < g_*$ (i.e., $t > t_*$), the diffusion-controlled decrease with time of the already-small fermion density is further significantly slowed down compared to Eq. (15). If we stop QA once g_* is reached, n_* gives the approximate solution of the annealing problem. Unexpectedly, the dependence of n_* and g_* on $|\dot{g}|$ is nonmonotonic, see Fig. 2. The optimal (minimal with respect to $|\dot{g}|$) value of n_* is

$$n_{\text{opt}} \approx [8\pi k\alpha^2/c_D\beta^3]z_{\text{opt}}^{3/2}, \quad (18)$$

where $z_{\text{opt}} \equiv \beta(1 - g_{\text{opt}}) \approx \log[\mu(\beta/\alpha)^2]$ is the value of z_* where n_* is optimal. The optimal speed is

$$|\dot{g}|_{\text{opt}} \approx (64k\pi^2 J\alpha^3/c_D\beta^5\hbar) \ln(\beta^2/\alpha^2)^{1/2}. \quad (19)$$

Equation (9) suggests that, in the considered dissipative system, QA can be started at the critical point. Then the time $z_{\text{opt}}/\beta|\dot{g}|_{\text{opt}}$ to reach g_{opt} is a small portion of the total time to reach $g = 0$, which is $|\dot{g}|_{\text{opt}}^{-1}$. The density n_{opt} is extremely small for weak coupling, $\alpha \ll 1$, and low temperatures, $\beta \gg 1$, and it rapidly decreases with decreasing α and $k_B T/J$.

The evolution of the fermion density for $t > t_*$ can be roughly estimated from the scaling equation $\langle \dot{n} \rangle = -k'D(g)\langle n \rangle^3$, cf. [36], where $k' \sim 1$. Because of the sharp decrease of $D(g)$ with increasing $1 - g$, the solution of this equation for $1 - g = \mathcal{O}(1)$ weakly depends on $g(t)$. For the optimal speed (19) such saturation density is $\langle n \rangle \sim n_{\text{opt}}/\ln(\beta/\alpha) \ll n_{\text{opt}}$.

It is instructive to compare the optimal speed (19) with the speed $|\dot{g}|_{\text{KZ}}$ that would lead to the same saturation density, $n_{\text{opt}}/\ln(\beta/\alpha) = n_{\text{KZ}}$, due to the Kibble-Zurek mechanism of the creation of excitations in the absence of coupling to the environment. From Eqs. (3) and (19),

$$\dot{g}_{\text{opt}}/\dot{g}_{\text{KZ}} \propto (\beta/\alpha) \ln(\beta/\alpha)^2 \gg 1. \quad (20)$$

Therefore, the time it takes to reach the approximate solution (18) in a closed quantum system is much larger than in our case.

It is instructive also to compare $|\dot{g}|_{\text{opt}}$ with the speed of annealing based on the classical Glauber dynamics [26]. In this dynamics, for $k_B T \ll J$ excitations in the Ising spin chain are eliminated through diffusion of kinks. If the transition rate for a kink to move to a neighboring site is w_G and the initial density of the kinks is ~ 1 , the time t_{class} to reach density $n \ll 1$ is $(8\pi w_G n^2)^{-1}$ [26]. In terms of our model, the uncertainty relation imposes a limitation $w_G \ll J/\hbar$. Therefore the ratio of the times to reach $n_{\text{opt}}/\ln(\beta/\alpha)$ via classical and quantum diffusion is very large, $\sim t_{\text{class}}|\dot{g}|_{\text{opt}} \propto \beta/\alpha \gg 1$.

The results demonstrate that quantum diffusion near the critical point provides an important mechanism of the speed-up of QA. The diffusion occurs over states that are large quantum superpositions of spin configurations

separated by the Hamming distance $\sim \beta g [\alpha(1-g)]^{-1} \gg 1$ of the order of the mean free path of a fermion. The bottleneck of QA in an open system can be imposed by the sharp slowing-down of the diffusion behind the critical region. The crossover to slow excitation recombination is accompanied by the onset of significant spatial fluctuations of the excitation density even in the absence of disorder. At the crossover, the residual density of excitations nonmonotonically depend on the quantum annealing rate $|\dot{g}|$. Its minimum provides the optimal value of the rate. This value scales with the coupling constant and temperature as $\alpha^3 T^5$, and the optimal excitation density is $\propto \alpha^2 T^3$. Importantly, the optimal speed $|\dot{g}|_{\text{opt}}$ is independent of the system size.

For our simple but nontrivial example of QA, attaining the approximate solution [40] via the quantum-diffusion-mediated process is faster than via classical diffusion or the closed-system QA. One might expect that, in higher-dimensional systems, quantum diffusion over extended states could provide an efficient route to finding approximate solutions in the presence of disorder above the many-body mobility edge [41].

This work was supported in part by the Office of the Director of National Intelligence (ODNI), Intelligence Advanced Research Projects Activity (IARPA), via IAA 145483, by the AFRL Information Directorate under Grant No. F4HBKC4162G001, and by NASA (Sponsor Award No. NNX12AK33A). D. V. and A. P.-O. were also supported in part by the Sandia National Laboratory AQUARIUS project. M. I. D. is grateful to the NASA Ames Research Center for the warm hospitality and partial support during his sabbatical.

*smelyan@google.com

†dykman@pa.msu.edu

- [1] T. Kadowaki and H. Nishimori, *Phys. Rev. E* **58**, 5355 (1998).
- [2] J. Brooke *et al.*, *Science* **284**, 779 (1999).
- [3] E. Farhi, J. Goldstone, S. Gutmann, J. Lapan, A. Lundgren, and D. Preda, *Science* **292**, 472 (2001).
- [4] A. Das and B. K. Chakrabarti, in *Quantum Annealing and Related Optimization Methods* Vol. 679 (Springer, Berlin, 2005).
- [5] M. H. S. Amin, C. J. S. Truncik, and D. V. Averin, *Phys. Rev. A* **80**, 022303 (2009).
- [6] M. W. Johnson *et al.*, *Nature (London)* **473**, 194 (2011).
- [7] N. G. Dickson *et al.*, *Nat. Commun.* **4**, 1903 (2013).
- [8] G. E. Santoro *et al.*, *Science* **295**, 2427 (2002).
- [9] S. Morita and H. Nishimori, *J. Math. Phys. (N.Y.)* **49**, 125210 (2008).
- [10] E. Crosson and A. W. Harrow, in IEEE 57th Annual Symposium on Foundations of Computer Science (2016), p. 714, <http://ieeexplore.ieee.org/abstract/document/7782986>.
- [11] M. B. Hastings, *Quantum Inf. Comput.* **13**, 1038 (2013).
- [12] B. Heim, T. F. Ronnow, S. V. Isakov, and M. Troyer, *Science* **348**, 215 (2015).
- [13] J. A. Smolin and G. Smith, *Front. Phys.* **2**, 52 (2014).
- [14] S. V. Isakov, G. Mazzola, V. N. Smelyanskiy, Z. Jiang, S. Boixo, H. Neven, and M. Troyer, *Phys. Rev. Lett.* **117**, 180402 (2016).
- [15] S. Muthukrishnan, T. Albash, and D. A. Lidar, *Phys. Rev. X* **6**, 031010 (2016).
- [16] S. Mandra, Z. Zhu, W. Wang, A. Perdomo-Ortiz, and H. G. Katzgraber, *Phys. Rev. A* **94**, 022337 (2016).
- [17] *Quantum Tunneling in Condensed Media*, edited by Y. Kagan and A. J. Leggett (North-Holland, Amsterdam, 1992).
- [18] T. W. B. Kibble, *J. Phys. A* **9**, 1387 (1976).
- [19] W. H. Zurek, *Nature (London)* **317**, 505 (1985).
- [20] D. Patanè, A. Silva, L. Amico, R. Fazio, and G. E. Santoro, *Phys. Rev. Lett.* **101**, 175701 (2008).
- [21] D. Patanè, L. Amico, A. Silva, R. Fazio, and G. E. Santoro, *Phys. Rev. B* **80**, 024302 (2009).
- [22] P. P. Orth, I. Stanic, and K. Le Hur, *Phys. Rev. A* **77**, 051601 (R) (2008).
- [23] H. Schwager, J. I. Cirac, and G. Giedke, *Phys. Rev. A* **87**, 022110 (2013).
- [24] A. W. Carr and M. Saffman, *Phys. Rev. Lett.* **111**, 033607 (2013).
- [25] O. Viehmann, J. von Delft, and F. Marquardt, *Phys. Rev. Lett.* **110**, 030601 (2013).
- [26] R. Glauber, *J. Math. Phys. (N.Y.)* **4**, 294 (1963).
- [27] S. Sachdev, *Quantum Phase Transitions* (Cambridge University Press, Cambridge, 1999).
- [28] E. Lieb, T. Schultz, and D. Mattis, *Ann. Phys. (N.Y.)* **16**, 407 (1961).
- [29] J. Dziarmaga, *Phys. Rev. Lett.* **95**, 245701 (2005).
- [30] See Supplemental Material at <http://link.aps.org/supplemental/10.1103/PhysRevLett.118.066802>, which includes Refs. [30–36], for details on the quantum kinetic equation, on the diffusion equation, on the renormalization of the fermion spectrum and on the crossover from the mean field regime to the diffusion limited regime.
- [31] A. O. Caldeira and A. J. Leggett, *Ann. Phys. (N.Y.)* **149**, 374 (1983).
- [32] D. Ben Avraham, M. Burschka, and C. Doering, *J. Stat. Phys.* **60**, 695 (1990).
- [33] V. Privman, C. R. Doering, and H. L. Frisch, *Phys. Rev. E* **48**, 846 (1993).
- [34] D. C. Mattis and M. L. Glasser, *Rev. Mod. Phys.* **70**, 979 (1998).
- [35] J. Allam, M. T. Sajjad, R. Sutton, K. Litvinenko, Z. Wang, S. Siddique, Q.-H. Yang, W. H. Loh, and T. Brown, *Phys. Rev. Lett.* **111**, 197401 (2013).
- [36] U. C. Tauber, *Critical Dynamics: A Field Theory Approach to Equilibrium and Non-Equilibrium Scaling Behavior* (Cambridge University Press, Cambridge, England, 2014).
- [37] M. Smoluchowsky, *Zur Didaktik der Physik und Chemie: Vorträge auf der Tagung für Didaktik der Physik/Chemie* **92**, 129 (1917).
- [38] G. Stefanucci and R. van Leeuwen, *Nonequilibrium Many Body Theory of Quantum Systems* (Cambridge University Press, Cambridge, 2013).
- [39] A. Altland and B. Simons, *Condensed Matter Field Theory* (Cambridge University Press, Cambridge, 2010).
- [40] E. Farhi, J. Goldstone, and S. Gutmann, [arXiv:1411.4028](https://arxiv.org/abs/1411.4028).
- [41] C. R. Laumann, A. Pal, and A. Scardicchio, *Phys. Rev. Lett.* **113**, 200405 (2014).

Supplemental Material for the paper: Quantum annealing via environment-mediated quantum diffusion

Vadim N. Smelyanskiy,¹ Davide Venturelli,^{2,3} Alejandro Perdomo-Ortiz,^{4,3} Sergey Knysh,^{5,3} and Mark I. Dykman⁶

¹Google, Venice, CA 90291

²USRA Research Institute for Advanced Computer Science (RIACS), Mountain View CA 94043

³NASA Ames Research Center, Mail Stop 269-1, Moffett Field CA 94035-1000

⁴University of California Santa Cruz, University Affiliated Research Center at NASA Ames

⁵Stinger Ghaffarian Technologies Inc., 7701 Greenbelt Rd., Suite 400, Greenbelt, MD 20770

⁶Department of Physics and Astronomy, Michigan State University, East Lansing, MI 48824-232

(Dated: January 5, 2017)

I. QUANTUM KINETIC EQUATION IN THE SINGLE-FERMION APPROXIMATION

In this section we briefly outline the starting point of the analysis, the Boltzmann equation for the fermion density matrix in the standard single-fermion approximation, and show that, as the system evolves, there emerges a separation of time scales between the rates of intraband scattering and the much slower rates of generation and recombination of fermions.

The problem of the dynamics of fermions coupled to phonons is a standard problem of the solid state physics [1]. If the coupling is weak, the fermion dynamics is often described by the Boltzmann equation. In this equation, correlations in the fermion system are disregarded. Another major assumption is that the characteristic duration of fermion scattering by phonons is short compared to the reciprocal scattering rate, which is determined by the coupling strength. In the problem considered in the main text, the fermion energy counted off from the bottom of the band is $k_B T$, and the typical duration of scattering is $\hbar/k_B T$. It is much smaller than the reciprocal scattering rate for the small coupling constant α .

The Boltzmann equation is Markovian and is formulated in terms of the coupling-induced transitions between the states of the fermions. For weak coupling, the rates of these transitions can be found in the Born approximation. The equation takes on a particularly simple form for a spatially uniform system, where the Wigner probability density $\rho_W(x, k) = \rho_k/N$ is independent of the coordinate x and just gives the probability density per unit length to find a fermion with the wave vector k ; we remind that the fermions are on a chain with N sites and the period of the chain is set equal to 1. The Boltzmann equation then reads

$$\frac{\partial \rho_k}{\partial t} = \mathcal{L}_k^{(0)}[\rho] + \mathcal{L}_k^{(1)}[\rho], \quad (1)$$

$$\mathcal{L}_k^{(0)}[\rho] = \sum_q \left(W_{qk}^{+-} (1 - \rho_k) \rho_q - W_{kq}^{+-} \rho_k (1 - \rho_q) \right)$$

$$\mathcal{L}_k^{(1)}[\rho] = \sum_q \left(W_{kq}^{--} (1 - \rho_k) (1 - \rho_q) - W_{kq}^{++} \rho_k \rho_q \right)$$

Here operator $\mathcal{L}^{(0)}$ describes inelastic intraband scattering, where a fermion makes a transition between states

with different wave numbers k , cf. Fig. 1 of the main text. The rate of a transition $k \rightarrow q$ is W_{kq}^{+-} . Operator $\mathcal{L}^{(1)}$ describes a two-fermion generation and recombination processes. The rates of these processes are $\propto W_{kq}^{--}$ and $\propto W_{kq}^{++}$, respectively. The transition rates are given by Eq. (5) of the main text.

For a fixed scaled transverse field g , Eq. (1) has a stationary solution given by the Fermi-Dirac distribution with zero chemical potential, $\rho_k = 1/[\exp(2J\epsilon_k/k_B T) + 1]$. In addition to the standard assumptions regarding the Boltzmann equation, in deriving Eq. (1) we assumed that, for varying g , the reciprocal duration of scattering is small compared to the QA rate, $k_B T/\hbar \gg |\dot{g}|$.

Unlike the scattering rates W_{kq}^{+-} , the rates $W_{kq}^{\mu\mu}$ (with $\mu = +$ or $\mu = -$) depend exponentially strongly on the relation between the energy gap $\Delta = 2J|1 - g|$ and $k_B T$. At the initial stage of QA, the energy gap is $\Delta \gg k_B T$ and the system is mostly frozen in its ground state, because fermion generation is suppressed, $W_{kq}^{--} \propto \exp(-2\Delta/k_B T)$. As the critical region $\Delta \lesssim k_B T$ is traversed, fermions with energies $\lesssim k_B T$ become thermally excited (and are potentially also excited via the Kibble-Zurek mechanism, which in the considered case of small $|\dot{g}|$ gives less excitations).

After the critical point is passed, the system again enters the semiclassical region $\Delta \gg k_B T$. The energy dispersion law becomes parabolic near the bottom of the band, with energy $2J\epsilon_k$,

$$\epsilon_k = 1 - g + (2J)^{-1} \frac{\hbar^2 k^2}{2m_e}, \quad m_e = \hbar^2 |1 - g| / 2Jg \quad (2)$$

(m_e is the fermion effective mass). Fermions with thermal energy have a typical wave number

$$k_{\text{th}} = [(1 - g)/\beta g]^{1/2}, \quad \beta = 2J/k_B T. \quad (3)$$

Since in the semiclassical region the two-fermion generation rate W_{kq}^{--} is exponentially small, the fermion population decreases. A key observation is that fermion annihilation requires a two-fermion collision with rate $W_{kq}^{++} \rho_k \rho_q$. Therefore it also slows down in the semiclassical regime. In contrast, the rate of intraband scattering described by the operator $\mathcal{L}_k^{(0)}$ in Eq. (1) has terms linear in ρ_k , which do not contain exponentially small factors.

Therefore intraband transitions are faster than generation and recombination.

The physical picture of the semiclassical dynamics is that, because of the intraband scattering, there is first established thermal distribution within the fermion band. The total fermion population changes on a longer time scale due to interband processes. If we keep only the intraband scattering terms in Eq. (1) and take into account that, for low fermion densities the system is nondegenerate, this equation takes the form

$$\frac{\partial \rho_k}{\partial t} \simeq \sum_q L_{kq}^{(0)} \rho_q, \quad L_{kq}^{(0)} = W_{qk}^{+-} - \delta_{kq} \sum_{k'} W_{kk'}^{+-}. \quad (4)$$

In the limit of a long chain, $N \gg 1$, and for $\beta^{-1} \ll |1 - g| \ll 1$, we introduce a scale-free integral kernel,

$$L_{kq}^{(0)} = \tau_r^{-1} \bar{L}_{KQ}^{(0)}, \quad K = k/k_{\text{th}}. \quad (5)$$

Here, τ_r^{-1} is the relaxation rate introduced in Eq. (7) of the main text, k_{th} is defined in Eq. (3), and

$$\begin{aligned} \bar{L}_{KQ}^{(0)} &= W_{KQ} - \delta(K - Q) \int dK' W_{KK'}, \quad (6) \\ W_{KQ} &= \frac{1}{2}(Q^2 - K^2) \{1 - \exp[-(Q^2 - K^2)/2]\}^{-1}. \end{aligned}$$

In writing this expression we took into account that the fermion energy dispersion law is parabolic.

A direct calculation shows that the eigenvalues e_m of $\bar{L}^{(0)}$ are non-positive. The maximal eigenvalue $e_0 = 0$ corresponds to the right eigenstate, which is the stationary solution of Eq. (4),

$$\rho_k = \frac{\langle n \rangle}{n_{\text{th}}} e^{-\beta \epsilon_k}, \quad n_{\text{th}} = \frac{1}{N} \sum_k e^{-\beta \epsilon_k}. \quad (7)$$

Equation (7) describes a quasi-equilibrium thermal distribution over fermion momenta; $\langle n \rangle$ is the spatially-independent fermion density (the angular brackets are introduced for the further analysis, where we will be considering spatial fluctuations); n_{th} is the thermal equilibrium density.

One further finds from the analysis of the eigenvalues of the operator $\bar{L}^{(0)}$ that its eigenvalues $e_{m>0}$ form a continuous spectrum (in the limit of $N \rightarrow \infty$) with a gap given by the first nonzero eigenvalue $e_1 = -6.6$. The rate $\tau_r^{-1}|e_1|$ is the typical relaxation rate of fermion momenta. It increases with the distance $1 - g \propto \Delta$ from the critical point.

The density $\langle n \rangle$ varies on the time scale $t \gg \tau_r$. An equation describing the slow time evolution of $\langle n \rangle$ in the neglect of spatial nonuniformity and correlations can be found by substituting expression (7) into the full Boltzmann equation (1) and performing summation over the momentum k in this equation. However, this approximation breaks down for low densities due to density fluctuations, as indicated in the main text.

II. DIFFUSION EQUATION

In this section we derive the diffusion equation, which describes the density fluctuations in the single-particle approximation. In our model the interaction between the particles comes from recombination and generation. If these processes are slow, the full quantum kinetic equation for the single-particle Wigner probability distribution $\rho_W(x, k, t) = \frac{1}{2\pi} \int_{-\infty}^{\infty} dp \langle \eta_{k+p/2}^\dagger(t) \eta_{k-p/2}(t) \rangle e^{-ipx}$ has the standard form of Eq. (6) of the main text, in which we now keep only the single-particle term,

$$\frac{\partial \rho_W(x, k)}{\partial t} + \frac{2J}{\hbar} \frac{\partial \rho_W(x, k)}{\partial x} \frac{\partial \epsilon_k}{\partial k} = \mathcal{L}^{(0)}[\rho_W(x, k)], \quad (8)$$

where the superoperator $\mathcal{L}^{(0)}[\rho_W(x, k)]$ has the same form as the collision term in Eq. (4), which for convenience we write here in the integral form,

$$\begin{aligned} \mathcal{L}^{(0)}[\rho_W(x, k)] &= \int_{-\infty}^{\infty} dq w_{qk} \rho_W(x, q) \\ &\quad - \rho_W(x, k) \int_{-\infty}^{\infty} dq w_{kq}, \quad (9) \end{aligned}$$

Here, for $\beta^{-1} \ll |1 - g| \ll 1$ the transition rates are

$$w_{kq} = \frac{4\alpha J}{\hbar\beta} W_{KQ}, \quad (10)$$

where the dimensionless rates W_{KQ} are given in Eq. (6), $k = Kk_{\text{th}}$. The rate w_{kq} is symmetric with respect to the inversion of the sign of the wave vectors k, q ,

$$w_{kq} \approx w_{|k||q|}. \quad (11)$$

The stationary solution of Eq. (9) is given by the spatially-uniform Boltzmann distribution over the fermion momentum,

$$\rho_W^{(0)}(k) = Z^{-1} \exp[-(\Delta/k_B T) - \frac{1}{2}K^2]. \quad (12)$$

Here $Z = \int_{-\infty}^{\infty} dk \exp(-\beta \epsilon_k)$ [the scaled energy ϵ_k is given in Eq. (2)]; the distribution (11) is normalized on unit density of fermions.

An important physical argument is that the time evolution of the fermion probability distribution with respect to momentum is fast, it occurs over time $\sim \tau_r$. The evolution of the spatial distribution (the coordinate-dependent part of ρ_W) is much slower. To find this slow evolution, we seek the time-dependent solution of Eq. (9) for a weakly spatially nonuniform distribution $\rho_W(x, k, t)$ as a sum of symmetric and anti-symmetric terms with respect to k , with the symmetric part being of the Boltzmann form,

$$\rho_W(x, k, t) = n(x, t) \rho_W^{(0)}(k) + \rho_W^{(1)}(x, k, t), \quad (13)$$

where

$$n(x, t) = \int_{-\infty}^{\infty} dk \rho_W(x, k, t), \quad (14)$$

is the spatially dependent fermion density and $\rho_W^{(1)}(x, k, t) = -\rho_W^{(1)}(x, -k, t)$ is a term that corresponds to a non-zero current,

$$\begin{aligned} j(x, t) &= \int_{-\infty}^{\infty} dk \frac{2J}{\hbar} \frac{d\epsilon_k}{dk} \rho_W(x, k, t), \\ &= \int_{-\infty}^{\infty} dk \frac{2J}{\hbar} \frac{d\epsilon_k}{dk} \rho_W^{(1)}(x, k, t). \end{aligned} \quad (15)$$

If we now substitute Eq. (13) into Eq. (9) and separate symmetric and anti-symmetric terms in k , we obtain

$$\frac{\partial n(x, t)}{\partial t} \rho_W^{(0)}(k) + \frac{2J}{\hbar} \frac{d\epsilon_k}{dk} \frac{\partial \rho_W^{(1)}(x, k, t)}{\partial x} = 0, \quad (16)$$

and

$$\frac{\partial \rho_W^{(1)}(x, k, t)}{\partial t} + \frac{2J}{\hbar} \frac{d\epsilon_k}{dk} \frac{\partial n}{\partial x} \rho_W^{(0)}(k) = -\tau_s^{-1}(k) \rho_W^{(1)}(x, k, t), \quad (17)$$

where

$$\tau_s^{-1}(k) = \int_{-\infty}^{\infty} dq w_{kq}. \quad (18)$$

In Eq. (16) we used that $\int dq w_{qk} \rho_W^{(1)}(q, x, t) = 0$ due to the symmetry property (11). This equation corresponds to a standard relaxation time approximation in the transport theory, which is simplified in the considered here symmetric one-dimensional case.

Integrating (16) over k and using (15), we obtain the continuity equation

$$\frac{\partial n(x, t)}{\partial t} + \frac{\partial j(x, t)}{\partial x} = 0. \quad (19)$$

Taking into account that the momentum relaxation time is small compared to the time over which the density $n(x, t)$ evolves, for time $t \gg \tau_s$ we obtain a quasi-stationary solution of Eq. (17) for $\rho_W^{(1)}$,

$$\rho_W^{(1)}(x, k, t) = -\frac{\partial n(x, t)}{\partial x} \tau_s(k) \rho_W^{(0)}(k) \frac{2J}{\hbar} \frac{d\epsilon_k}{dk}. \quad (20)$$

The current then is just a diffusion current,

$$j(x, t) = -D \frac{\partial n(x, t)}{\partial x}, \quad (21)$$

where D is the diffusion coefficient,

$$D = \int_{-\infty}^{\infty} dk \rho_W^{(0)}(k) \tau_s(k) \left(\frac{2J}{\hbar} \frac{d\epsilon_k}{dk} \right)^2. \quad (22)$$

The continuity equation (19) now takes the form of a diffusion equation for the spatial fermion density $n(x, t)$,

$$\frac{\partial n(x, t)}{\partial t} = D \frac{\partial^2 n(x, t)}{\partial x^2} \quad (23)$$

The explicit form of the diffusion coefficient D in the semiclassical region, which follows from Eqs. (10), (18) and (22), is given in Eq. (11) of the main text.

We can now write explicitly the condition of the applicability of the single-particle approximation. This condition is that the recombination rate $w(g)n^2$ is slow compared to the diffusion rate [the recombination rate per unit density $w(g)$ is given by Eq. (13) of the main text]. The diffusion rate has to be calculated as the inverse time to diffuse over an interparticle distance, which from Eq. (23) is $\sim Dn^3$. Therefore the single-particle approximation applies for $Dn \gg w$, i.e., for not too small particle density. This condition gives the density n_* in Eq. (16) of the main text.

III. RENORMALIZATION OF THE FERMION SPECTRUM

In addition to fermion scattering, coupling of the fermions to the bosonic field leads to a renormalization of the fermion energy spectrum (the polaronic effect) and fermion mixing. For weak coupling, the corresponding effects are small. It is the small renormalization condition that imposes a constraint on the coupling strength. We specify it here for the Ohmic-coupling, where the density of states of the bosonic bath weighted with the coupling is $2\hbar^{-2} \sum_{\gamma} \lambda_{\gamma n}^2 \delta(\omega - \omega_{\gamma}) = \alpha \omega \exp(-\omega/\omega_c)$ for all lattice sites n .

The effect of the Ohmic spin-boson coupling in an Ising chain is different from the case of a particle in a potential well coupled to bosons, where the coupling-induced energy renormalization could be incorporated into the potential [2]. In the case of a spin chain, the polaronic energy shift depends on the fermion energy and also on the transverse magnetic field, which varies in time.

Special attention has to be paid to the case of a very large parameter ω_c . A simple perturbation theory shown below diverges if it is extended to bosons with energies $\hbar\omega_{\gamma} \rightarrow \infty$. However, it is clear on physical grounds that high-energy bosons with $\hbar\omega_{\gamma} \gg 2J$ should adiabatically follow the spin dynamics. For large ω_c , we introduce a cutoff frequency ω_{cutoff} such that $\omega_{\text{cutoff}} \gg 2J/\hbar$ but $\omega_{\text{cutoff}} < \omega_c$. The effect of bosons with $\omega_{\gamma} \geq \omega_{\text{cutoff}}$ can be accounted for by the standard polaronic transformation

$$U = \exp \left[\sum_{\gamma, n} \sigma_n^x \frac{\lambda_{\gamma n}}{\hbar\omega_{\gamma}} (b_{\gamma n} - b_{\gamma n}^{\dagger}) \Theta(\omega_{\gamma} - \omega_{\text{cutoff}}) \right]$$

where $\Theta(x)$ is the step function. This transformation eliminates the coupling of σ_n^x to such bosons. It shows that the major effect of the high-energy bosons is the renormalization of the Ising energy $J \rightarrow J \exp(-W)$ with $W \sim 2\alpha \log(\omega_c/\omega_{\text{cutoff}})$. We assume that such renormalization has been done and that $W \ll 1$.

After the high-energy bosons are eliminated (if they were present initially), the analysis of the renormalization of the fermion energy can be done using the explicit

form of the parameters of the coupling Hamiltonian in the main text,

$$\begin{aligned} c_{kk'} &= 2N^{-1/2} \cos[(\theta_k + \theta_{k'})/2], \\ s_{kk'} &= iN^{-1/2} \sin[(\theta_k + \theta_{k'})/2]. \end{aligned} \quad (24)$$

If we disregard the contribution of thermal bosons, to the second order in λ_γ the expression for the polaronic energy shift $2J\Sigma_k$ of a fermion with wave vector k has a standard form, with

$$\begin{aligned} \Sigma_k &= \frac{\alpha}{2} \text{v.p.} \int \bar{\omega} \exp[-\bar{\omega}/\bar{\omega}_c] d\bar{\omega} \\ &\times \sum_{k'} \left[\frac{|c_{kk'}|^2}{\epsilon_k - \epsilon_{k'} - \bar{\omega}} + \frac{4|s_{kk'}|^2}{\epsilon_k + \epsilon_{k'} - \bar{\omega}} \right], \end{aligned} \quad (25)$$

where v.p. indicates the principal value of the integral and $\bar{\omega}_c = \hbar\omega_c/2J$. For $\omega_c \lesssim 2J/\hbar$, the integration over $\bar{\omega}$ goes from $\bar{\omega} = 0$ to ∞ . On the other hand, if $\omega_c \gg 2J/\hbar$, the upper limit of the integral is $\bar{\omega}_{\text{cutoff}} = \hbar\omega_{\text{cutoff}}/2J$.

The coupling-induced mixing corresponds to an extra term in the fermion Hamiltonian of the form of $2J \sum_k \Sigma_k^{(c)} \eta_k^\dagger \eta_{-k}^\dagger + \text{H.c.}$ If we disregard the contribution from thermally excited bosons,

$$\begin{aligned} \Sigma_k^{(c)} &= \frac{\alpha}{2} \text{v.p.} \int \bar{\omega} \exp[-\bar{\omega}/\bar{\omega}_c] d\bar{\omega} \sum_{k'} s_{kk'} c_{kk'} \\ &\times [(\epsilon_k - \epsilon_{k'} - \bar{\omega})^{-1} - (\epsilon_k + \epsilon_{k'} - \bar{\omega})^{-1}]. \end{aligned} \quad (26)$$

The limits of the integral over $\bar{\omega}$ are the same as in Eq. (25).

It is important that the coupling to bosons does not lead to mixing of long-wavelength ($k \rightarrow 0$) excitations. This is because $\epsilon_{-k'} = \epsilon_{k'}$, whereas $s_{kk'} c_{kk'} \propto \sin(\theta_k + \theta_{k'})$ changes sign for $k' \rightarrow -k'$ in the limit $k \rightarrow 0$.

Of interest to us is the parameter range close to the critical point, $|g - 1| \ll 1$, and a range of the scaled fermion energies $\epsilon_k \ll 1$. Because such fermions have small k , the coupling practically does not mix fermions with opposite momenta. The leading-order scaled energy shift for $\epsilon_k \ll 1$ is $\Sigma_k \sim -\alpha\bar{\omega}_{\text{cutoff}}$ for $\bar{\omega}_c \gg 1$, i.e., for broadband bosons. On the other hand, for narrow-band bosons (compared to the Ising coupling energy J), i.e., for $\bar{\omega}_c \ll 1$, we have $\Sigma_k \sim -\alpha\bar{\omega}_c^2$ for $k \rightarrow 0$. We note that the condition $\bar{\omega}_c \ll 1$ is compatible with the conditions $\bar{\omega}_c \gg 1/\beta, 1 - g_{\text{opt}}$ used in the main text to describe relaxation of long-wavelength fermions; here $g_{\text{opt}} = 1 - x_{\text{opt}}/\beta$, where x_{opt} is given by Eq. (17) in the main text; $1 - g_{\text{opt}} \ll 1$.

The shift Σ_k for $k \rightarrow 0$ determines the shift in the critical value of the control parameter g . The shape of the

spectrum of long-wavelength fermions near the critical point is not changed by the renormalization (25). Indeed, it can be seen from Eq. (25) that $\Sigma_k \approx \Sigma_{k \rightarrow 0} + C\epsilon_k$. Constant C is $\sim \alpha \log \bar{\omega}_{\text{cutoff}}$ for $\bar{\omega}_c \gg 1$ and is $\sim \alpha\bar{\omega}_c^2$ for $\bar{\omega}_c \ll 1$.

IV. CROSSOVER FROM THE MEAN FIELD REGIME TO THE DIFFUSION LIMITED REGIME

In this section we provide an alternative estimate of the fermion density where spatial fluctuations of the fermion density cannot be disregarded and the recombination rate becomes diffusion-limited. Such crossover has been studied in a number of papers [4–8] where the diffusion coefficient and the recombination rate were assumed constant. In the mean-field regime described by the rate equation [Eq. (12) of the main text] these assumptions lead to a linear increase of the reciprocal density in time in the large-time limit, if generation is neglected. In our problem, the fermion density decreases logarithmically slowly, Eq. (15) of the main text, while the diffusion rate $D \propto (1 - g)^{-3/2}$ [Eq. (11) of the main text] sharply falls off in time.

To estimate the time and density where there occurs the crossover in our problem, we extend the Smoluchowski argument for the diffusion-limited reaction rate [9] to systems with time-dependent diffusion coefficient. We consider a random spatial configuration of fermions at an instant τ . Typically, a given fermion is separated from other fermions on the both sides by “empty” intervals [4] of size $\ell(\tau) = \langle n \rangle^{-1}(\tau)$. For $t > \tau$, the fermion diffuses toward the boundaries of this interval, which are moving themselves due to fermion recombination. The typical distance over which the particle diffuses is $\ell_D(t, \tau) = [\int_\tau^t dt' D(t')]^{1/2}$, whereas the interparticle distance varies as $\ell(t) - \ell(\tau) = \int_\tau^t dt' w(g(t')) dt'$, where the recombination rate per particle w is defined in Eq. (13) of the main text.

For recombination to occur, functions $\ell_D(t, \tau)$ and $\ell(t) \equiv \langle n \rangle^{-1}(t)$ should coincide at some time t . Using the explicitly known time dependence of D and w , we can see that the distance between the particles increases in time faster than the diffusion distance $\ell_D(t, \tau)$. The maximal time t_* where one can still have $\ell_D(t, \tau) = \ell(t)$ is given by equation $d(\ell_D^2(t, \tau))/dt = d\ell^2(t)/dt$. It corresponds to the curves $\ell_D(t, \tau)$ and $\ell(t)$ touching at time t_* . This condition leads to equation

$$n(t_*) = kw(t_*)/D(t_*), \quad k \sim 1,$$

which is the crossover condition discussed in the main text.

[1] A. Altland and B. Simons, *Condensed Matter Field Theory*, Cambridge University Press (Cambridge, 2010).

[2] A. O. Caldeira and A. J. Leggett, *Ann. Phys. (N.Y.)* **149**, 374 (1983).

- [3] D. Patan et al., Phys. Rev. Lett. **101**, 175701 (2008); Phys. Rev **B 80**, 024302 (2009).
- [4] D. Ben Avraham, M. Burschka, and C. Doering, J. Stat. Phys. **60**, 695 (1990).
- [5] V. Privman, C. R. Doering, and H. L. Frisch, Phys. Rev. E, **48**, 846 (1993)
- [6] D. C. Mattis and M. L. Glasser, Rev. Mod. Phys., **70**, 979 (1998).
- [7] J. Allam, M. T. Sajjad, R. Sutton, K. Litvinenko, Z. Wang, S. Siddique, Q.-H. Yang, W. H. Loh, and T. Brown, Phys. Rev. Lett. **111**, 197401 (2013)
- [8] Uwe C. Tauber, Critical Dynamics: A Field Theory Approach to Equilibrium and Non-Equilibrium Scaling Behavior (Cambridge University Press, Cambridge 2014).
- [9] M. Smoluchowsky, Z. Phys. Chem. **92**, 129 (1917).